Monthly Notices
of the
ROYAL ASTRONOMICAL SOCIETY

Mon. Not. R. Astron. Soc. **425,** 1633–1639 (2012) doi:10.1111/j.1365-2966.2012.21530.x

Search for sub-parsec massive binary black holes through line diagnosis – II

C. Montuori,[1⋆] M. Dotti,[2] F. Haardt,[1,3] M. Colpi[2] and R. Decarli[4]

[1] *Università degli Studi dell'Insubria, Via Valleggio 11, 22100 Como, Italy*
[2] *Università degli Studi di Milano-Bicocca, Piazza della Scienza 3, 20126 Milano, Italy*
[3] *INFN, Sezione di Milano-Bicocca, Piazza della Scienza 3, 20126 Milano, Italy*
[4] *Max-Planck Institut für Astronomie, Königstuhl 17, 69117 Heidelberg, Germany*

Accepted 2012 June 15. Received 2012 May 16

ABSTRACT

Massive black hole (BH) binaries at sub-parsec separations may display in their spectra anomalously small flux ratios between the Mg II and C IV broad emission lines, i.e. $F_{\rm Mg\,II}/F_{\rm C\,IV} \lesssim 0.1$, due to the erosion of the broad line region around the active, secondary BH, by the tidal field of the primary. In Paper I, we focused on broad lines emitted by gas bound to the lighter accreting member of a binary when the binary is at the centre of a hollow density region (the gap) inside a circum-binary disc. The main aim of this new study is to explore the potential contribution to the broad line emission by the circum-binary disc and by gaseous streams flowing towards the BH through the gap. We carry out a post-process analysis of data extracted from a smoothed particle hydrodynamic simulation of a circum-binary disc around a BH binary. Our main result is that the Mg II to C IV flux ratio can be reduced to ∼0.1 within an interval of sub-parsec binary separations of the order of $a \sim (0.01\text{–}0.2)(f_{\rm Edd}/0.1)^{1/2}$ pc corresponding to orbital periods of $\sim(20\text{–}200)(f_{\rm Edd}/0.1)^{3/4}$ yr for a secondary BH mass in the range $M_2 \sim 10^7$–$10^9\,{\rm M}_\odot$ and a binary mass ratio of 0.3. At closer separations this ratio increases to values that are indistinguishable from the case of a single active galactic nucleus (typically $F_{\rm Mg\,II}/F_{\rm C\,IV} \sim 0.3-0.4$) because of the contribution to the Mg II line from gas in the circum-binary disc.

Key words: black hole physics – galaxies: kinematics and dynamics – galaxies: nuclei – quasars: general.

1 INTRODUCTION

Recent progress in the observational search of active galactic nuclei (AGN) with peculiar features led to the discovery of a sizable number of active black hole (BH) pairs in galaxies undergoing a merger, dubbed as dual AGN. These pairs are observed when the two galaxies are in the early stage of a merger, at separations in excess of several kpc (e.g. Comerford et al. 2009; Green et al. 2010; Liu et al. 2010; Fu et al. 2011; Shields et al. 2012). The dual BHs are expected to evolve into a close pair, as they sink in the gravitational potential of the new galaxy. At about a few parsec, the BHs form a Keplerian binary, and this occurs when their mass exceeds the mass of stars and gas enclosed in their orbit (see Colpi & Dotti 2011, for a review). This phase and the phase of subsequent hardening due to the interaction of the stellar/gaseous background are still difficult to observe. At such close separations, the binary (if both BHs are active) would not be identified as a dual source due to an insufficient spatial resolution.

The discovery of bona fide BH binaries (BHBs) is important as it represents a fundamental test for current models of galaxy formation: BHBs are signposts of galactic mergers and thus of the cosmic assembly of substructures. Nonetheless, convincing observational evidence of close BHBs in galactic nuclei is still missing with a few exceptions. Two compact double radio nuclei are observed in the core of the galaxy 0402+379 on scales of ∼7 pc (Rodriguez et al. 2006), and signatures of a Keplerian motion of a sub-pc BHB have been claimed in OJ287 (see Valtonen et al. 2008 and references therein).

Spectroscopic search of BHBs is a promising technique for the search of such elusive sources. The BHs in a close binary revolve around the common centre of mass with a velocity that can highly exceed the velocity of gas and stars far out in the gravitational potential of the background galaxy, and this may generate a velocity offset among atomic emission lines. Taking advantage of the wealth of spectroscopic data made publicly available, thanks to the Sloan Sky Digital Survey (SDSS; York et al. 2000), different groups developed systematic strategies focused on the selection of AGN spectra displaying multiple sets of narrow and broad emission lines (BELs) with relative Doppler shifts $\gtrsim$1000 km s^{-1} (e.g. Eracleous

⋆E-mail: carmen.montuori@uninsubria.it

© 2012 The Authors
Monthly Notices of the Royal Astronomical Society © 2012 RAS

et al. 2012; Tsalmantza et al. 2011; Tsalmantza & Hogg 2012). Substantial velocity offsets between the two sets of emission lines, respectively associated with the host galaxy reference frame and the gas bound to the single BH, potentially mark the orbital motion of the active member of the binary system in the galactic nucleus. Follow-up campaigns revealing periodic changes in the observed Doppler-shifted lines are necessary in order to firmly favour the binary hypothesis against other possible physical scenarios such as a recoiling BH resulting from a BHB coalescence, a double-peaked emitter or a chance superposition along the line of sight. Considering that the orbital period of a sub-pc BHB can be as long as a few 100 years, the spectral monitoring of these sources is rather long. A further disadvantage of this direct Doppler-shift technique is that the spectroscopic search is limited to a redshift of $z \lesssim 0.8$ as at higher redshifts all the most important narrow emission lines fall out of the optical range covered by the survey.

In Montuori et al. (2011, hereafter Paper I), we devised a tool for exploring potential spectral signatures of sub-pc BHBs at redshift $z \sim 2$, where BHBs should be frequent according to the present hierarchical cosmological model. The explored scenario was that of a binary, surrounded by a circum-binary disc, that after clearing a gap, i.e. a low-density hollow region in the midst of the disc, has confined its activity around the secondary BH fed by material inflowing from the inner edge of the disc (e.g. Artymovicz & Lubow 1994; Ivanov, Papaloizou & Polnarev 1999; Hayasaki, Mineshige & Sudou 2007; Hayasaki, Mineshige & Ho 2008; Cuadra et al. 2009). We assumed that a small-scale accretion disc is maintained around the secondary BH throughout the binary orbital decay induced by the external torques from the circum-binary disc or by the emission of gravitational waves (e.g. Haiman, Kocsis & Menou 2009). In Paper I we noticed that under these conditions BEL clouds orbiting around the active BH suffer erosion inside the gap due to the tidal truncation at the Roche lobe surface, resulting in a sizable reduction in the flux ratio between lines of low and high ionization potentials relative to the typical values observed for isolated AGN. In particular, it was found that sub-parsec BHBs could be potentially identified in the archives of current automatic surveys selecting AGN spectra characterized by a flux ratio between the Mg II and the C IV lines ($F_{\rm Mg\,II}/F_{\rm C\,IV}$) below $\lesssim$0.1.

In Paper I, the contribution to the different BELs from illuminated gas not bound to the secondary, active BH was neglected. In this paper, we improve upon our earlier investigation by studying the contribution to the BELs resulting from reprocessing of BH radiation by the gas of the circum-binary disc and by gas streams in the gap region flowing towards the BHB. In particular, we explore when and how the ratio $F_{\rm Mg\,II}/F_{\rm C\,IV}$ varies in response to changes in the spatial distribution of the broad line emitting gas as the binary hardens.

Sections 2 and 3 describe how we extend our previous result, guided by a qualitative analysis, and later by a more quantitative study. In Section 4 we present the results of this analysis, carried out with data taken from smoothed particle hydrodynamic (SPH) numerical simulations. Discussion and conclusions are given in Section 5.

2 KEY SPATIAL SCALES ALONG BINARY EVOLUTION

In order to overcome some of the simplifying assumptions made in our exploratory paper (Paper I), we consider here the potentially observable contribution from gas in the circum-binary disc surrounding the BHB. We start with a schematic view of the spatial scales

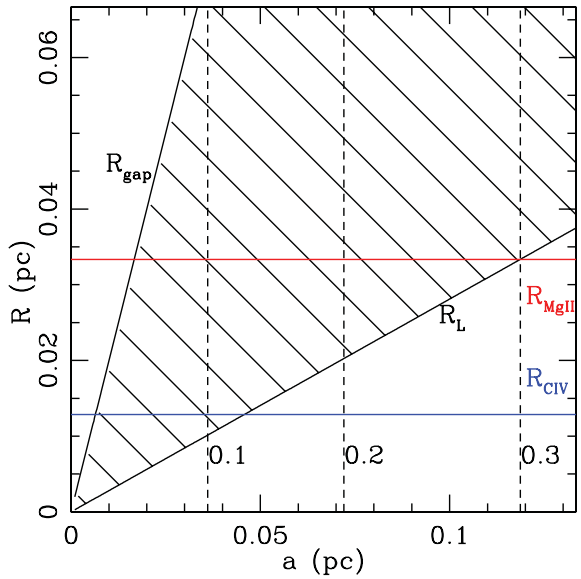

Figure 1. Schematic view of the most relevant spatial scales in our BHB model as a function of a. The binary is interacting with a circum-binary disc, and the secondary BH is the only active member of the system. The binary mass ratio is $q = 0.3$, and the secondary BH mass is $M_2 = 10^8\,{\rm M}_\odot$. The two solid black lines represent the radii of the Roche lobe ($R_{\rm L}$) around the secondary BH and the radius of the inner edge of the circum-binary disc ($R_{\rm gap}$), respectively. The shaded area in between these two lines corresponds to the lower density region in the central part of the circum-binary disc, i.e. the gap. The red and blue horizontal lines correspond to the values of $R_{\rm BLR}$ computed from the radius–luminosity relationship for the Mg II and the C IV emission lines, respectively. The secondary BH is assumed to be active as an AGN with an Eddington ratio of 0.1. The vertical dashed lines mark the orbital separations corresponding to different values of $F_{\rm Mg\,II}/F_{\rm C\,IV}$ computed for the material bound to the active BH, orbiting inside $R_{\rm L}$ (see the text for more details).

relevant to our binary evolutionary model. Two characteristic radii are present: the Roche lobe radius $R_{\rm L}$ around the secondary, only active BH and the inner edge of the circum-binary disc $R_{\rm gap}$. The Roche radius $R_{\rm L} \sim 0.49\,a\,q^{2/3}/[0.6q^{2/3} + \ln(1 + q^{1/3})]$ (Eggleton 1983) and $R_{\rm gap} = 2a$ (e.g. Artymovicz & Lubow 1994) are plotted in Fig. 1 as a function of the binary orbital separation a, for a circular BHB with mass ratio $q = 0.3$ and mass of the secondary $M_2 = 10^8\,{\rm M}_\odot$. The shaded area corresponds to the gap region between $R_{\rm L}$ and $R_{\rm gap}$, while the horizontal lines correspond to the values of $R_{\rm BLR}$ calculated from the following radius–luminosity relations for the C IV ($R_{\rm C\,IV}$, in blue; Kaspi et al. 2007) and the Mg II ($R_{\rm Mg\,II}$, in red; McLure & Jarvis 2002):

$$R_{\rm C\,IV} = 0.014 \times \left(\lambda L_{1350}/10^{43}\,{\rm erg\,s^{-1}}\right)^{0.55}\ {\rm pc} \quad (1)$$

$$R_{\rm Mg\,II} = 0.022 \times \left(\lambda L_{3000}/10^{44}\,{\rm erg\,s^{-1}}\right)^{0.47}\ {\rm pc}, \quad (2)$$

where λL_{1350} and λL_{3000} are the continuum luminosities at 1350 and 3000 Å. We consider the case of a secondary BH shining with a constant Eddington ratio set to $f_{\rm Edd} = 0.1$. The vertical dotted lines mark the orbital separations corresponding to different values of $F_{\rm Mg\,II}/F_{\rm C\,IV}$ (0.1, 0.2 and 0.3 as indicated in the figure) for the lines emitted by the gas of the broad line region (BLR) located inside $R_{\rm L}$. These orbital separations are computed as described in Paper I. In particular, the emission from the BLR around the secondary BH is modelled according to the locally optimal cloud model (e.g. Baldwin et al. 1995), adopting a power law with index set to -1 for the cloud's radial distance from the active source, and a uniform

distribution for the cloud's density at each radius. The hydrogen number density is set in the range $10^9 \leq n_{\rm H} \leq 6 \times 10^{12}\,{\rm cm}^{-3}$ so that at $a_0 \simeq 0.12\,{\rm pc}$, our starting point where $R_{\rm L}$ coincides with $R_{\rm Mg\,II}$, $F_{\rm Mg\,II}/F_{\rm C\,IV}$ is consistent with the typical values observed for standard AGN, i.e. ∼0.3–0.4 (see fig. 4 in Paper I). Moving towards smaller BHB separations, we highlight the occurrence of intervals possibly characterized by different observational signatures. As the binary separation shrinks, $R_{\rm L}$ becomes smaller than $R_{\rm Mg\,II}$. According to our previous results, this implies a reduction in the ratio $F_{\rm Mg\,II}/F_{\rm C\,IV}$ for the BELs associated with the BLR of the secondary BH. We consider the results of Paper I to be valid until the flux ratio drops to a value $F_{\rm Mg\,II}/F_{\rm C\,IV} \sim 0.1$ at an orbital separation of $a \simeq 0.04\,{\rm pc}$, corresponding to a period of $P \simeq 40\,{\rm yr}$, for the selected binary parameters. The contribution coming from the material not bound to the secondary active BH can be still neglected at these separations considering that: (i) the gas density in the gap region is expected to be much lower than the density relative to standard BLRs, and the BELs are efficiently reprocessed only at high densities; and (ii) the inner edge of the circum-binary disc $R_{\rm gap}$ is located at a distance $> 2R_{\rm Mg\,II}$ so that the ionizing flux reaching the higher density material associated with the outer circum-binary disc would be more than an order of magnitude lower relative to the flux intercepted by the gas bound to the active source.

As the semimajor axis shortens further, this spectroscopic signature is not expected to be a good tracer of the presence of a sub-pc BHB, since the additional contribution of the circum-binary disc cannot be any longer neglected, yielding an increase in $F_{\rm Mg\,II}/F_{\rm C\,IV}$. At intermediate separations of the order of $a \simeq 0.02\,{\rm pc}$, where $R_{\rm gap} \approx R_{\rm Mg\,II}$, $F_{\rm Mg\,II}/F_{\rm C\,IV}$, could be even higher than that typically observed for isolated AGN since the circum-binary disc could start to contribute significantly to the Mg II line while the C IV emission flux could be still reduced relative to the case of a single AGN since $R_{\rm L} < R_{\rm C\,IV} < R_{\rm gap}$. At the smallest orbital separations, of the order of $a < 0.01\,{\rm pc}$, where $R_{\rm gap} \lesssim R_{\rm C\,IV}$, the higher density gas of the circum-binary disc could efficiently reprocess both the C IV and the Mg II emission lines, bringing $F_{\rm Mg\,II}/F_{\rm C\,IV}$ back to the values observed for standard BLRs.

3 REPROCESSING OF RADIATION IN SIMULATED CIRCUM-BINARY DISCS

In Section 2 we qualitatively showed that the flux ratio of the Mg II and C VI emission lines varies with BHB separation, and that this change may not be monotonic with decreasing a, due to the contribution to the line flux from dense gas present in the circum-binary disc, depending on the relative position of the two critical radii $R_{\rm CVI}$ and $R_{\rm Mg\,II}$ with respect to $R_{\rm gap}$ and $R_{\rm L}$.

To proceed more quantitatively in our analysis, we model the spectroscopic signatures of a close BHB by applying here a simple line radiative transfer algorithm on data extracted from a simulated model of a circum-binary gas disc. The model self-consistently accounts for the presence of a low (but finite) density region, i.e. the gap, and of gas streams that leaking out through the inner edge of the disc are accreted by the binary.

In particular, we consider the numerical results presented by Sesana et al. (2012, hereafter S12) who used a modified version of the SPH code GADGET-2 (Springel 2005; Cuadra et al. 2009) to model the complex feeding process of a BHB embedded in a coplanar, corotating circum-binary accretion disc. The orbital separation in the simulation, $a \simeq 0.01\,{\rm pc}$, is in the interval appropriate to test our working hypothesis, namely that the line fluxes from Mg II and C VI can have a contribution from dense gas in the circum-binary disc. At the considered orbital separation, the simulated binary system is still dynamically coupled with the circum-binary disc, while its orbital decay is dominated by the emission of gravitational waves (see S12 and references therein).

We map the gas density field on a cubic, three-dimensional coarse grid,[1] and in the following we refer to the cubic grid elements as pixels. Pixels are then exposed to the ionizing radiation originating from gas accreting in the putative small-scale disc around the secondary BH. The small-scale accretion disc is assumed to be coplanar with the binary, and the ionizing emission is modelled adopting a cosine-like dilution along the disc axis to mimic thermal emission from an optically thick (geometrically thin) accretion flow (e.g. Shakura & Sunyaev 1973; Ivanov et al. 1999). In the SPH simulation at hand the gas accretion rate on to the BH is given by summing over all particles crossing the BH sink radius in a time-step. In our analysis, we select simulation snapshots corresponding to the secondary BH radiating with a luminosity of 0.1 Eddington luminosity (assuming 10 per cent radiative efficiency). Then, for all simulation pixels, the gas ionization state is computed using the code CLOUDY (version 08.00; Ferland et al. 1998). We adopt the AGN SED template stored in the code, scaled to the appropriate level given by the coordinates of the considered pixel. The ionization state of the gas is determined moving from the innermost pixels to the outer region along straight ray paths. To trace the cumulative effect of radiation absorption along a ray path, we make a net distinction between pixels that are optically thick and pixels that optically thin to the H I ionizing continuum. We assume that a pixel is not reached by ionizing radiation if at least one optically thick pixel is met along a ray. Our treatment is clearly a simplified description of the real radiative transfer, as we assume complete (zero) absorption for $\tau \geq 1$ ($\tau < 1$). However, this procedure greatly facilitates the analysis process, and at the same time captures the basic feature of sharp ionization fronts expected in the circum-binary gas.

The next step is to model the BELs. A self-consistent model for the BLR is still lacking as it is poorly constrained by the observations. Despite these limitations, the origin of the BELs is generally attributed to compact, dense condensations rapidly moving in a hotter intercloud medium (e.g. Osterbrock & Ferland 2006). Though the density of such unresolved clouds (estimated to be $\gtrsim 10^{10}\,{\rm cm}^{-3}$) is well above the maximum density given by our SPH simulation, we can use the gas distribution determined in the SPH simulation as a physically motivated 'background' density field to model the spatial distribution of the BEL clouds. With this aim, we select the densest ($n_{\rm H} > 10^8\,{\rm cm}^{-3}$) ionized regions of the circum-binary disc and of the streams flowing from its inner-edge, and there we superimpose a distribution of gas overdensities mimicking the BEL clouds. Operatively, we add a gaseous clump in all illuminated pixels whose hydrogen number density is above a given threshold. Such limiting value is set so that the total number of pixels embedding BEL clumps do not exceed 10 per cent of the total number of ionized pixels. The density of each BEL clump is set randomly from a uniform distribution in the range $10^8 \leq n_{\rm H} \leq 10^{12}\,{\rm cm}^{-3}$. We further assume that the clumps filling factor is $\ll 1$, so that the cumulative shielding effect along ray paths can be neglected. As discussed in the following section, we manage to check the consistency of our expectations discussed in Section 2 without any other constraint on the distribution of such BEL clumps.

[1] The results of our analysis are not significantly affected by the choice of the grid geometry and resolution.

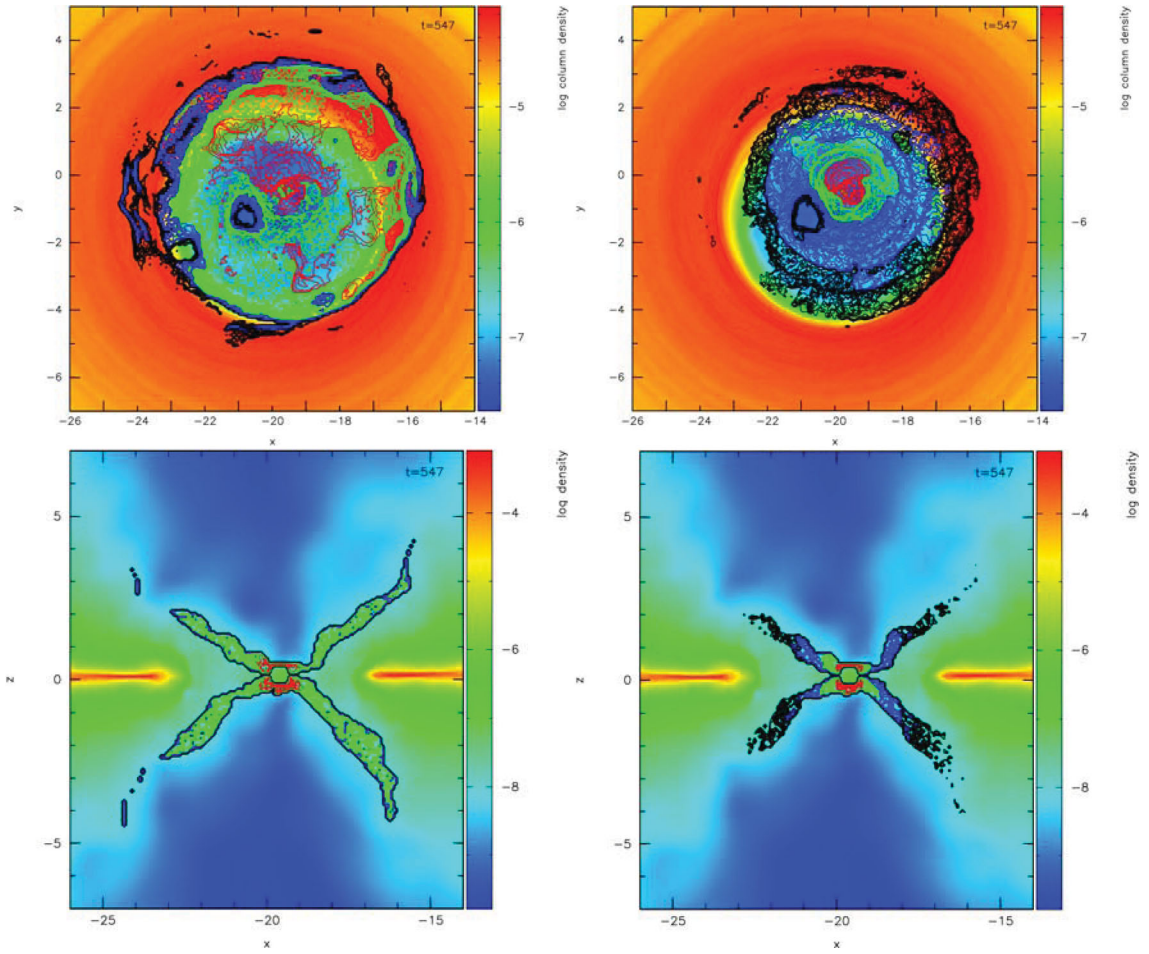

Figure 2. Contour plots of the Mg II (left-hand panels) and C IV (right-hand panels) emission line intensity superimposed on the density map of a snapshot taken from an SPH numerical simulation of a massive BHB embedded in a coplanar, corotating circum-binary disc. The upper panels show the projected intensity map for a face-on view relative to binary orbital plane superimposed on the surface density map. The lower panels correspond to an edge-on view with a slice of the intensity map overlaid on a slice of the density map, both taken in the $z - x$ plane at the y-coordinate of the secondary BH. The secondary coordinates are $(-19.6, -0.9, 0.1)$. The lower density gas of the gap region has green and blue colours in the density maps while the higher density gas of the surrounding circum-binary disc is coloured in red and yellow. Similarly the colour scale of the emission line contour levels spans two order of magnitudes, uniformly spaced in the logarithm, starting from the maximum intensity value in the map with red going to green, blue and black. These plots are obtained following the post-process analysis procedure described in more detail in the text.

Once BEL clumps are added, we use again CLOUDY to compute their line emission properties. As a final remark, we caution that we do not model the emission coming from the gas orbiting inside the Roche lobe of the secondary. The numerical resolution is not high enough to describe the properties of the material located at radii $\ll 0.5\,a$. We note that the main interest of our work here is to compute the broad line emission from the material not bound to the active BH, but rather bound to the binary, in order to test our qualitative expectations.

4 RESULTS

In this section we describe the results from a simulation of a close BHB with $a \simeq 0.01$ pc, a secondary BH with mass $M_2 \simeq 10^8\,\mathrm{M}_\odot$ and mass ratio $q \simeq 0.3$, surrounded by a coplanar, corotating circum-binary disc with a gap. In particular, we consider a snapshot where the secondary active BH accretes with $f_{\rm Edd} \simeq 0.1$ (we adopt a radiative efficiency of 0.1.). As discussed in Section 2, the binary model implies that $R_{\rm C\,IV} \lesssim R_{\rm gap} < R_{\rm Mg\,II}$. Therefore we expect that the gas in the circum-binary disc would give an important contribution to the BELs.

In Fig. 2, we show our results superimposing the intensity contour plot of the Mg II and the C IV lines on the density map of the selected snapshot. As described in the previous section, the BELs clouds are distributed on top of the cubic grid adding a gaseous clump to those illuminated pixels whose hydrogen number density is $n_{\rm H} \geq 10^8\,\mathrm{cm}^{-3}$. These pixels are located in the gap region and in a thin layer above the circum-binary disc midplane, within a radius $r \lesssim 2R_{\rm Mg\,II}$ (where $2R_{\rm Mg\,II} \simeq 0.065$ pc, corresponding to $\simeq 6$ internal unit lengths of the simulation). As shown in Fig. 2, the emission line intensity maps follow the spatial distribution of the gaseous clumps. We obtain $F_{\rm Mg\,II}/F_{\rm C\,IV} \gtrsim 0.2$ for the emission coming from the gaseous overdensities. The relative contribution to the C IV and the Mg II lines coming from the gap region is of the order of 67 and 34 per cent.

In order to verify that our results are not affected by the details of the post-process procedure, we perform a second analysis starting from the same snapshot but considering an isotropic ionizing source. Although the number of illuminated pixels is 30 per cent larger in

this case, the results are consistent with the previous analysis. The emission coming from the gap region increases since the ionizing flux is not zero in the direction perpendicular to the polar axis. In this case we have $F_{\rm Mg\,II}/F_{\rm C\,IV} \gtrsim 0.15$ and the relative contribution to the C IV and Mg II lines from the gaseous clumps in the central cavity is of the order of 73 and 25 per cent, respectively. We point out that the simplified procedure adopted for the distribution of the overdensities does not take into account that the formation of the gaseous clumps might be disfavoured in the gap region, characterized by lower densities and higher temperatures. For this reason $F_{\rm Mg\,II}/F_{\rm C\,IV}$ could be higher than that computed with our analysis since we might be overestimating the contribution to the C IV line coming from the clumps closer to the ionizing source.

According to Section 2, we expect to select BHB candidates with a peculiarly reduced value of $F_{\rm Mg\,II}/F_{\rm C\,IV}$ when the circum-binary disc is still too far from the active source and does not give a significant contribution to the BELs. As shown in Fig. 1, $F_{\rm Mg\,II}/F_{\rm C\,IV}$ computed for the BLR around the secondary BH is reduced to a value of $\simeq$0.1 at an orbital distance of the order of $a \simeq 0.04$ pc, while the inner edge of the circum-binary disc $R_{\rm gap}$ is located far out at radii $\simeq 2R_{\rm Mg\,II}$. In order to quantitatively check such predictions we perform an additional test using the same snapshot and rescaling the unit length by a factor of 4 so that the orbital separation of the simulated binary system is $a \simeq 0.04$ pc. According to equation (14) of S12, the rescaling keeps a disc-to-binary mass ratio of a few per cent, still consistent with the value of 1.5×10^{-2} assumed in the simulation for $a \simeq 0.01$ pc. Now we can compare the emission fluxes obtained with the distribution of gaseous clumps considered for the $a \simeq 0.01$ pc case with the emission fluxes computed for an equal number of clumps (with the same total mass and densities) superimposed on the snapshot rescaled at $a \simeq 0.04$ pc. In particular, the gaseous clumps are added to the rescaled snapshot pixels that are ionized by the active source and whose number density is $n_{\rm H} > 5 \times 10^6\,{\rm cm}^{-3}$.

With this procedure we find that the contribution to the C IV and the Mg II fluxes from the circum-binary disc, at a binary separation of $a \simeq 0.04$ pc, is reduced relative to the case with $a \simeq 0.01$ pc by factors of $\simeq$10 and $\simeq$100, respectively. This is consistent with our expectations considering that on average the ionizing flux reaching the high-density clumps is in this case reduced by an order of magnitude. According to the model assumed for the cloud distribution in the BLR of the secondary BH, at the considered orbital separation the BELs flux reduction, relative to the fluxes computed at a_0, is of the order of 28 and 75 per cent for the C IV and the Mg II line, respectively. According to our results, the contribution from the outer disc to the C IV line can be neglected while that to the Mg II line corresponds to an increase of $\sim$10 per cent. Even considering this external emission, we obtain $F_{\rm Mg\,II}/F_{\rm C\,IV} \sim 0.15$ that is still reduced relative to its typical values for single AGN. This is consistent with our BHB selection criterion, as discussed in Paper I, of $F_{\rm Mg\,II}/F_{\rm C\,IV} \lesssim 0.1$ considering both the uncertainties in the calculations and in the BLR model.

5 DISCUSSION

Fig. 3 shows, as a function of the mass of the secondary active BH, the minimum and maximum values of the orbital period P (upper panel) and of the orbital velocity v_2 (lower panel) of the active BH relative to the binary centre of mass, within which we expect to select a BHB system from its peculiarly reduced value of $F_{\rm Mg\,II}/F_{\rm C\,IV}$. The corresponding BHB separations can be inferred

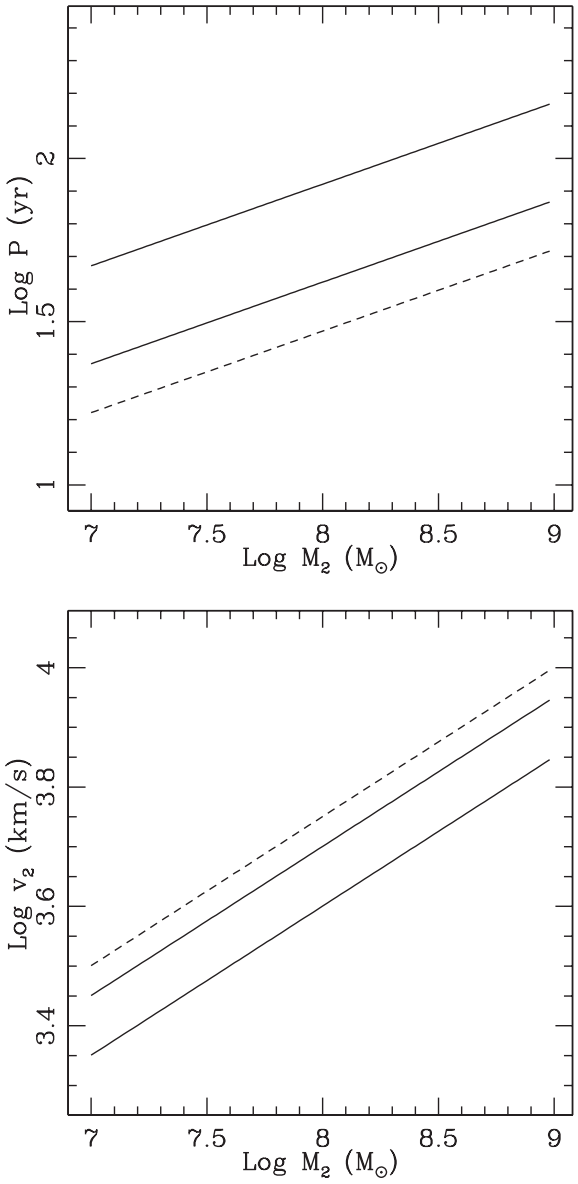

Figure 3. Range of orbital parameters of BHB candidates characterized by a peculiar value of $F_{\rm Mg\,II}/F_{\rm C\,IV}$. The orbital period P (upper panel) and the orbital velocity of the active BH v_2 (lower panel) are plotted as a function of the mass M_2 of the active BH. The BH is accreting with $f_{\rm Edd} = 0.1$, and the binary mass ratio is $q = 0.3$. Two different models for the BLR bound to the active BH are considered. Solid lines refer to the maximum orbital period (minimum orbital velocity) for the two considered BLR models. Dashed lines indicate the minimum period and the corresponding maximum orbital velocity. These parameters are the same for both BLR models (see text for details).

given the relation $a \simeq 0.08\,(M_2/10^8\,{\rm M}_\odot)^{1/3}(P/100\,{\rm yr})^{2/3}$ pc for a binary mass ratio of 0.3.

Relying on the results discussed in Section 4, the limiting values for P and v_2 are obtained requiring that: (i) $R_{\rm gap} \gtrsim 2R_{\rm Mg\,II}$, so that the circum-binary disc contributes to the Mg II line at most by 10 per cent relative to the typical BEL flux of a single AGN; (ii) $F_{\rm Mg\,II}/F_{\rm C\,IV} \lesssim 0.15$ even considering the additional contribution from the gas not bound to the active BH. We set the upper limit for $F_{\rm Mg\,II}/F_{\rm C\,IV}$ to 0.15 on the basis of the observed distribution inferred from $\simeq$6000 quasar spectra in the SDSS archive ($\simeq$90 per cent of the sources

© 2012 The Authors, MNRAS **425,** 1633–1639
Monthly Notices of the Royal Astronomical Society © 2012 RAS

have $F_{\rm Mg\,II}/F_{\rm C\,IV} > 0.15$; see fig. 4 of Paper I). Maximum periods (minimum velocities) depend on the way we model the BLR around the active BH. In the upper panel of Fig. 3 describing the run of P with M_2, the lower solid line refers to the BLR model considered in the previous sections, i.e. a uniform density distribution and a power law with index -1 for the radial distance distribution (hereafter Model A). The upper solid line corresponds to the case of a power law with index -0.5 for the radial distribution while the densities are set uniformly in the range $10^9 \leq n_{\rm H} \leq 2.5 \times 10^{12}{\rm cm}^{-3}$ (hereafter Model B). In the lower panel for v_2 the upper and lower solid lines refer to Models A and B, respectively. For Model B (which has a flatter radial distribution and a lower upper limit for the density range relative to Model A) the emission coming from the outer part of the BLR is more relevant and $F_{\rm Mg\,II}/F_{\rm C\,IV}$ can be significantly reduced also at higher orbital separations. However in Model B we notice that $F_{\rm Mg\,II}/F_{\rm C\,IV}$ computed at the starting orbital separation, corresponding to $R_{\rm L} = R_{\rm Mg\,II}$, is lower by a factor of ~ 0.8 because of the lower density assumed for the BLR clouds. Therefore we consider the maximum orbital values computed with Model B as upper limits. Moreover, for BLR clouds distributed uniformly in both radius and density, the effect of the flux ratio reduction would be even stronger than the models considered in the figure. In this case, however, the BEL fluxes would be so diminished as the orbital separation shrinks that the contribution from the external gas would be more effective in increasing $F_{\rm Mg\,II}/F_{\rm C\,IV}$ to its standard values. In this case, there would be a narrower range of orbital parameters suitable to observe a peculiar $F_{\rm Mg\,II}/F_{\rm C\,IV}$ because of the presence of a close BHB.

Solid and dashed lines in Fig. 3 scale as $M_2^{1/4}$. The scaling can be simply understood considering that the maximum and minimum orbital separations (thus the maximum and minimum P) correspond to a fixed ratio $R_{\rm L}/R_{\rm BLR}$. This means that $R_{\rm L,max/min} \propto f_{\rm Edd}^{1/2} M_2^{1/2}$ (see the $R_{\rm BLR}$–luminosity relations reported in Section 2), where the subscript $_{\rm max/min}$ refers to the maximum/minimum value of the parameter. Since $a \propto R_{\rm L}$, we obtain

$$P_{\rm max/min} \propto \left(\frac{a_{\rm max/min}^3}{M_2}\right)^{1/2} \propto \frac{\left(f_{\rm Edd}^{1/2} M_2^{1/2}\right)^{3/2}}{M_2^{1/2}} \propto M_2^{1/4} \qquad (3)$$

and

$$v_{2,\rm max/min} \propto \left(\frac{M_2}{a_{\rm min/max}}\right)^{1/2} \propto \left(\frac{M_2}{f_{\rm Edd}^{1/2} M_2^{1/2}}\right)^{1/2} \propto M_2^{1/4}. \qquad (4)$$

As noticed before, we are working under the assumption of a circular binary orbit so that there is a fixed relation between the Roche radius of the secondary BH and the binary semi-major axis. A number of numerical studies showed that the interaction with a circum-binary disc can bring the eccentricity of a binary system up to a constant saturation value which is fairly high, i.e. $e \sim 0.6$–0.8 (e.g. Cuadra et al. 2009; Roedig et al. 2011). The Roche lobe radius is ill-defined for an eccentric binary. On an eccentric orbit with $e \sim 0.6$, the active, secondary BH has an apocentre (pericentre) $\sim$1.6 ($\sim$0.4) times larger (smaller) than a circular orbit. Under these circumstances, the BLR of the secondary BH may have no time to re-expand after the truncation at the pericentric passage due to the characteristics of the periodic inflows of material on to the BHs. The analysis presented in Section 4 for the $a \simeq 0.01$ pc case would not be significantly affected by the precise value of the Roche lobe of the secondary BH. Indeed, $R_{\rm L} \lesssim 0.15\, R_{\rm Mg\,II}$ in both cases so that the circum-binary disc would still give the major contribution to the BELs.

Results are different when most of the emission comes from the material bound to the secondary BH, as in the $a \simeq 0.04$ pc case. In this case, if the BLR of the secondary BH does not expand after the pericentric passage, $F_{\rm Mg\,II}/F_{\rm C\,IV}$ would be that computed for a binary with a semimajor axis reduced by a factor of $\simeq 2.5$. Then, it could be possible to select binary candidates with longer orbital periods compared to the circular case. If instead the BLR expands to fill $R_{\rm L}$ at the apocentre the flux ratio reduction would be less significant. The chance to select a binary candidate before the circum-binary disc starts to contribute to the BELs would be lower, and more affected by the details of the BLR model.

6 SUMMARY AND CONCLUSIONS

In this work we pursue our investigation of new possible observable signatures associated with close massive BHBs interacting with a circum-binary disc. In Paper I, we proposed a technique based on the observation of a peculiarly reduced value of the flux ratio between two prominent BELs characterized by different ionization potentials, i.e. the C IV and the Mg II lines.

In this second work we addressed the robustness of the proposed criterion when the presence of the material surrounding the BHB is considered. In particular, we aimed at quantifying the effect on $F_{\rm Mg\,II}/F_{\rm C\,IV}$ of the circum-binary disc and the low-density gas in the gap. As in Paper I, we assumed a circular BHB with the secondary being the only active BH. We presented a qualitative estimate of the relative importance of the external contributions to the BEL fluxes at different orbital separations. We then tested our results with the post-process analysis of a SPH simulation of a BHB embedded in a circum-binary disc. The main result of our analysis can be summarized stating that we expect to select close massive BHBs because of a peculiarly reduced value of $F_{\rm Mg\,II}/F_{\rm C\,IV}$ for a limited range of sub-pc orbital separations. In this range the main contribution to the BELs comes from the tidally perturbed BLR bound to the secondary active BH. We notice that, although orbiting at very close separations, the BHBs characterized by a low $F_{\rm Mg\,II}/F_{\rm C\,IV}$ are expected to be in the long-lived disc-driven phase of the binary orbital migration (e.g. Haiman et al. 2009). At even closer separations, where the binary lifetimes are shorter due to the emission of gravitational waves, the line flux from the BLR of the secondary keeps on reducing, while the gas associated with the circum-binary disc starts to give a significant contribution to the BELs. This has two main consequences: (i) $F_{\rm Mg\,II}/F_{\rm C\,IV}$ rises up to the typical observed range for AGN, and (ii) the wavelengths of the BEL peaks are not expected to be related to the orbital motion of the active BH, in agreement with Shen & Loeb (2010) for a different BLR geometry.

ACKNOWLEDGMENTS

The authors thank Costanze Roedig, Alberto Sesana and Jorge Cuadra for useful discussions. MC is grateful to Costanze Roedig for the helpfulness in providing access to the results she obtained from the numerical simulations. MC, MD and FH are also thankful for the warm hospitality offered at the AEI in Berlin.

REFERENCES

Artymovicz P., Lubow S. H., 1994, ApJ, 421, 651
Baldwin J., Ferland G., Korista K., Verner D., 1995, ApJ, 455, L119
Colpi M., Dotti M., 2011, Adv. Sci. Lett., 4, 181

Comerford J. M., Griffith R. L., Gerke B. F., Cooper M. C., Newman J. A., Davis M., Stern D., 2009, ApJ, 702, L82
Cuadra J., Armitage P. J., Alexander R. D., Begelman M. C., 2009, MNRAS, 393, 1423
Eggleton P. P., 1983, ApJ, 268, 368
Eracleous M., Boroson T. A., Halpern J. P., Liu J., 2012, ApJS, 201, 23
Ferland G. J., Korista K. T., Verner D. A., Ferguson J. W., Kingdon J. B., Verner E. M., 1998, PASP, 110, 761
Fu H. et al., 2011, ApJ, 740, L44
Green P. J., Myers A. D., Barkhouse W. A., Mulchaey J. S., Bennert V. N., Cox T. J., Aldcroft T. L., Wrobel J. M., 2010, ApJ, 712, 762
Haiman Z., Kocsis B., Menou K., 2009, ApJ, 700, 1952
Hayasaki K., Mineshige S., Sudou H., 2007, PASJ, 59, 427
Hayasaki K., Mineshige S., Ho L. C., 2008, ApJ, 682, 1134
Ivanov P. B., Papaloizou J. C. B., Polnarev A. G., 1999, MNRAS, 307, 79
Kaspi S., Brandt W. N., Maoz D., Netzer H., Schneider D. P., Shemmer O., 2007, ApJ, 659, 997
Liu X., Greene J. E., Shen Y., Strauss M. A., 2010, ApJ, 715, L30
McLure R. J., Jarvis M. J., 2002, MNRAS, 337, 109
Montuori C., Dotti M., Colpi M., Decarli R., Haardt F., 2011, MNRAS, 412, 26 (Paper I)
Osterbrock D. E., Ferland G. J., 2006, in Osterbrock D. E., Ferland G. J., eds, Astrophysics of Gaseous Nebulae and Active Galactic Nuclei, 2nd edn. University Science Books, Sausalito, CA
Rodriguez C., Taylor G. B., Zavala R. T., Peck A. B., Pollack L. K., Romani R. W., 2006, ApJ, 646, 49
Roedig C., Dotti M., Sesana A., Cuadra J., Colpi M., 2011, MNRAS, 415, 3033
Sesana A., Roedig C., Reynolds M. T., Dotti M., 2012, MNRAS, 420, 860 (S12)
Shakura N. I., Sunyaev R. A., 1973, A&A, 24, 337
Shen Y., Loeb A., 2010, ApJ, 725, 249
Shields G. A., Rosario D. J., Junkkarinen V., Chapman S. C., Bonning E. W., Chiba T., 2012, ApJ, 744, 151
Springel V., 2005, MNRAS, 364, 1105
Tsalmantza P., Hogg D. W., 2012, ApJ, 753, 122
Tsalmantza P., Decarli R., Dotti M., Hogg D. W., 2011, ApJ, 738, 20
Valtonen M. J. et al., 2008, Nat, 452, 851
York D. G. et al., 2000, AJ, 120, 1579

This paper has been typeset from a TEX/LATEX file prepared by the author.

© 2012 The Authors, MNRAS **425,** 1633–1639
Monthly Notices of the Royal Astronomical Society © 2012 RAS